Available online at www.sciencedirect.com
ScienceDirect
Journal of the European Ceramic Society 28 (2008) 843–849
www.elsevier.com/locate/jeurceramsoc

Structure and electrical properties of $(Na_{0.5}Bi_{0.5})_{1-x}Ba_xTiO_3$ piezoelectric ceramics

Min Chen [a], Qing Xu [b,*], Bok Hee Kim [a,**], Byeong Kuk Ahn [a], Jung Hoon Ko [a], Woo Jin Kang [a], O. Jeong Nam [a]

[a] *Division of Advanced Materials Engineering, Hydrogen & Fuel Cell Research Center, Chonbuk National University, 1-664-14, Duckjin-dong, Duckjin-ku, Chonju, Chonbuk 561-756, South Korea*
[b] *School of Materials Science and Engineering, Wuhan University of Technology, Wuhan 430070, PR China*

Received 25 June 2007; received in revised form 5 August 2007; accepted 20 August 2007
Available online 22 October 2007

Abstract

$(Na_{0.5}Bi_{0.5})_{1-x}Ba_xTiO_3$ ceramics were synthesized by the citrate method and their structure and electrical properties were systematically investigated. The results of X-ray diffraction analysis revealed a MPB composition range of $x = 0.06$–0.10 for $(Na_{0.5}Bi_{0.5})_{1-x}Ba_xTiO_3$ system at room temperature. It was found that the piezoelectric and ferroelectric properties of $(Na_{0.5}Bi_{0.5})_{1-x}Ba_xTiO_3$ compositions near the MPB are rather sensitive to the phase composition and reach preferred values at $x = 0.07$, where the relative content of the tetragonal phase is substantially higher than that of the rhombohedral phases. $(Na_{0.5}Bi_{0.5})_{1-x}Ba_xTiO_3$ ceramics present a decrease diffusive factor (δ) with increasing $BaTiO_3$ content, implying a degradation of the relaxor feature and a transition from relaxor ferroelectrics to normal ferroelectrics.

Keywords: Citric method; Perovskite; Piezoelectricity; Lead-free

1. Introduction

Nowadays, there is an increasing interest of investigating lead-free piezoelectric materials from the viewpoint of environmental consideration. Sodium bismuth titanate, $(Na_{0.5}Bi_{0.5})TiO_3$ (NBT), has been regarded as a promising candidate for lead-free piezoelectric ceramics due to its strong ferroelectricity at room temperature.[1] However, NBT suffers from a poling problem because of its high coercive field ($E_c = 73$ kV/cm) and high conductivity, causing a difficulty in obtaining desired piezoelectric properties. To solve this problem, various NBT-based solid solutions have been developed.[2–5] Ceramics with good piezoelectric properties can be obtained by the partial substitution of A-site ions $(Na_{0.5}Bi_{0.5})^{2+}$ by Ba^{2+}, $(K_{0.5}Bi_{0.5})^{2+}$ and others.[6,7] However, NBT-based ceramics formed by the substitution of the B-site ion Ti^{4+} by Nb^{5+} or Fe^{3+},[4,8] display only a slight enhancement of their piezoelectric properties. Thus, it has been suggested that NBT is only A-site active in ABO_3 piezoelectric materials.[9] Hence, to further improve the piezoelectric properties of lead-free ceramics, it is necessary to develop the NBT-based solid solutions with A-site substitution. Among the solid solutions that have been developed so far, $(Na_{0.5}Bi_{0.5})_{1-x}Ba_xTiO_3$ (NBT–(x)BT) system has attracted considerable attention, because of the existence of a rhombohedral–tetragonal morphotropic phase boundary (MPB) near $x = 0.06$. Compared with other A-site substituted NBT-based solid solutions, NBT–(x)BT compositions near the MPB provide substantially improved poling and piezoelectric properties.[2,6]

On the other hand, NBT-based ceramics are usually fabricated by the conventional solid-state method. Recently, considerable research efforts have been devoted to the preparation of materials by various wet chemical methods, such as citrate method,[10] emulsion method,[11] hydrothermal process[12] and stearic acid gel route.[13] It was found that NBT-based ceramics made from powders synthesized by alternative methods exhibit improved sinterability, poling process and piezoelectric properties.[14] In the present study, NBT–(x)BT ceramics were produced by the

* Corresponding author. Tel.: +86 27 87863277; fax: +86 27 87864580.
** Corresponding author. Tel.: +82 63 2702380; fax: +82 63 2702386.
E-mail addresses: xuqing@mail.whut.edu.cn (Q. Xu), kimbh@chonbuk.ac.kr (B.H. Kim).

0955-2219/$ – see front matter © 2007 Elsevier Ltd. All rights reserved.
doi:10.1016/j.jeurceramsoc.2007.08.007

citrate method, and their structure and electrical properties were examined.

2. Experimental procedures

The powders with the nominal composition of $(Na_{0.5}Bi_{0.5})_{1-x}Ba_xTiO_3$ ($x = 0$, 0.02, 0.04, 0.06, 0.07, 0.08, 0.10, 0.12, 0.20) were synthesized by the citrate method. Reagent grade $NaNO_3$, $Bi(NO_3)_3{\bullet}5H_2O$, $Ba(NO_3)_2$, tetrabutyl titanate and citric acid were used as starting materials. Tetrabutyl titanate was first dissolved in citric acid solution and various nitrates were then added, followed by stirring to yield a transparent aqueous solution. The mole ratio of citric acid to the total metal cation content was 1.25. The precursor solution was heated to form a sol and subsequently a gel. The gel was calcined at 600 °C for 1 h in air. The details of the synthesis process have been described elsewhere.[15] The crystal structure of calcined powders with various BT concentrations was examined by a Rigaku D/MAX-RB X-ray diffractometer using Cu Kα radiation. The morphology of the calcined powders was observed using a Hitach S-4700 field emission scanning electron microscope (FESEM).

The calcined powders (100–200 nm) were pressed into discs with a diameter of 19 mm in diameter and thickness of 1 mm, and then sintered at 1150 °C for 2 h in air. The crystal structure of the ceramic specimens was investigated by a Philips X'Pert Pro X-ray diffractometer with a step size of 0.017° using Cu Kα radiation. The microstructure of the ceramic specimens was investigated by a Jeol JSM-5610LV scanning electron microscope (SEM). For the ceramic specimens, their thermally etched surfaces were used for SEM observation. The ceramic specimens were polished to ensure the flatness of their surface and painted with silver paste on both surfaces as electrodes. The dielectric properties were measured using an HP4294 impedance analyzer at 1 kHz. The dielectric constants (ε_r) of unpoled ceramics at room and elevated temperature were measured at 1, 10 and 100 kHz using a TH2818 automatic component analyzer. The specimens for measuring piezoelectric properties were poled in a silicon oil bath at 60 °C under 3.5 kV/mm for 15 min. The piezoelectric constant (d_{33}) was measured using a quasistatic d_{33} meter based on the Berlincourt method at 110 Hz. The electromechanical coupling factor (k_p), mechanical quality factor (Q_m) and frequency constant (N_p) were measured by the resonance–antiresonance method using an HP4294 impedance analyzer. The polarization–electric field (P–E) hysteresis loop was measured by a Radiant Precision workstation based on a standard Sawyer–Tower circuit at 50 Hz.

3. Results and discussion

Fig. 1 shows the X-ray diffraction (XRD) patterns of NBT–(x)BT ceramics in the 2θ ranges of 38–42° and 45–48°, respectively. The rhombohedral symmetry of pure NBT at room temperature is characterized by a (0 0 3)/(0 2 1) peak splitting between 38° and 42° and a single (2 0 2) peak between 45° and 48°. In Fig. 1(a), the (0 0 3)/(0 2 1) peak splitting is still

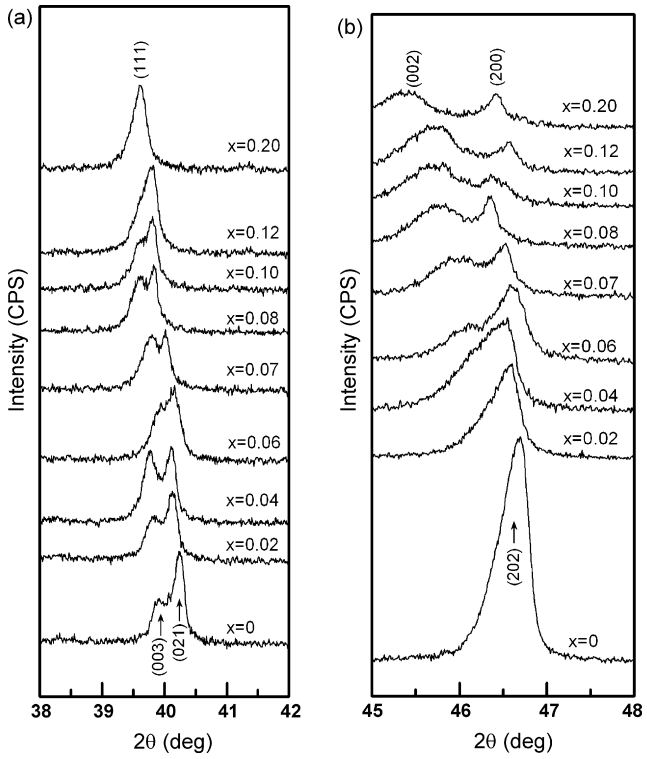

Fig. 1. XRD patterns of NBT–(x)BT ceramics in the 2θ ranges of (a) 38–42° and (b) 45–48°.

distinguishable until $x = 0.10$. In Fig. 1(b), a distinct peak splitting can be seen at $x \geq 0.06$ and beyond, corresponding to a tetragonal symmetry. Therefore, it can be inferred that the MPB of NBT–(x)BT ceramics lies in the composition range of $0.06 \leq x \leq 0.10$ at room temperature, where the rhombohedral and tetragonal phases coexist. Various compositional ranges of the MPB have been reported for NBT–(x)BT ceramics, such as $x = 0.06$–0.07[2] and $0.04 < x < 0.06$,[6] showing a slight difference between different studies. According to the theoretical model for the MPB in $Pb(Zr, Ti)O_3$ solid solution, the width of the MPB, Δx, is inversely proportional to the grain size of the ceramics.[16] Therefore, it is not surprising that the values of Δx obtained by different processing techniques are quite different. The result of this work is generally in agreement with those of previous studies.

Considering the gradual evolution of the XRD patterns from a single (2 0 2) peak, corresponding to a rhombohedral symmetry, to a (0 0 2)/(2 0 0) peak splitting, corresponding to a tetragonal symmetry, the splitting of the peaks for the MPB compositions can be ascribed to the simultaneous diffraction of the (0 0 2)/(2 0 2)/(2 0 0) planes. To characterize the phase compositions in a more quantitative way, the XRD patterns of the MPB compositions in the 2θ ranges of 45–48° were fitted into the (0 0 2)/(2 0 2)/(2 0 0) peaks by Peakfit software, based on the fitting results obtained for the $x = 0$ (rhombohedral) and $x = 0.20$ (tetragonal) compositions, as shown in Fig. 2. The data shows the Lorentzian deconvolution of the (0 0 2) and (2 0 0) peaks of the tetragonal phase and the (2 0 2) peak of the rhombohedral phase. The mole content of rhombohedral phase (M_R) can be

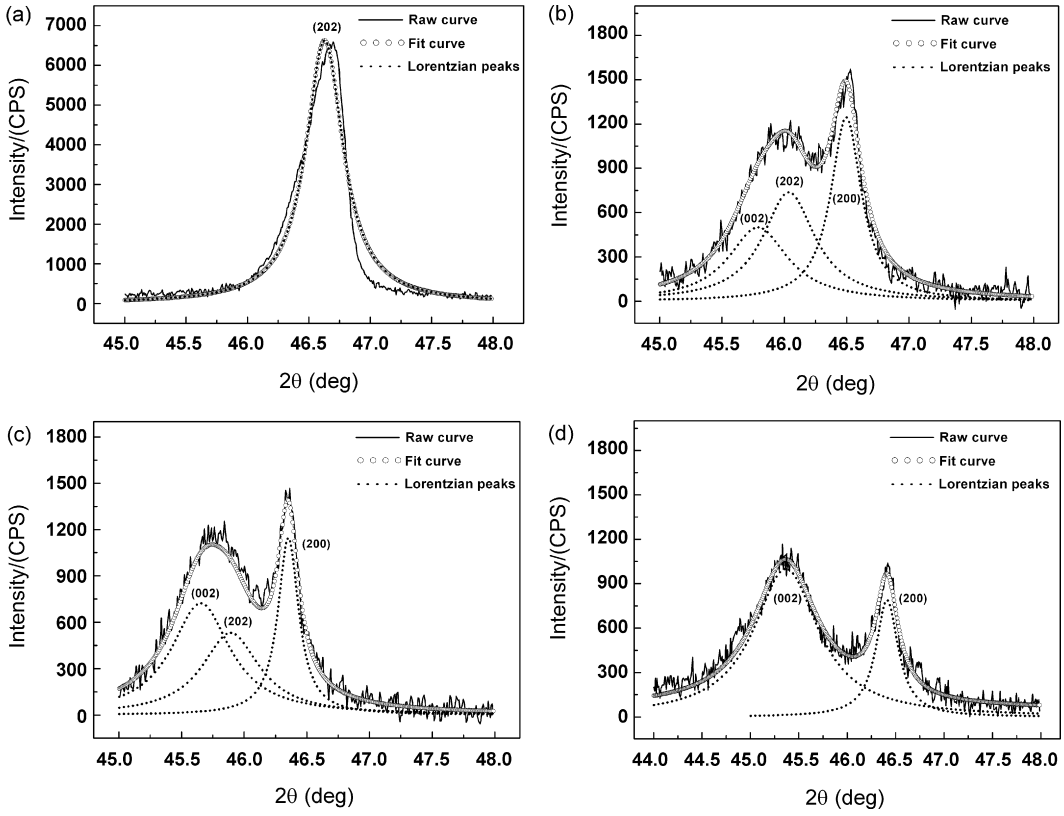

Fig. 2. XRD fitting patterns of NBT–(*x*)BT ceramics with (a) $x = 0$, (b) $x = 0.07$, (c) $x = 0.08$ and (d) $x = 0.20$.

obtained from the equation:

$$M_R = \text{area}(2\,0\,2)_R/(\text{area}(0\,0\,2)_T + \text{area}(2\,0\,0)_T + \text{area}(2\,0\,2)_R)$$

Table 1 shows the phase compositions of NBT–(*x*)BT ceramics, confirming that with increasing concentration of BT, the relative content of rhombohedral phase is gradually reduced.

Fig. 3 shows SEM micrographs of NBT–(*x*)BT ceramics. There is an obvious decrease of the grain size with increasing BT concentration, suggesting that dissolving BT into NBT inhibits the grain growth.

Fig. 4 shows the piezoelectric properties of NBT–(*x*)BT ceramics as a function of BT concentration. The piezoelectric constant (d_{33}) and electromechanical coupling factor (k_p) display a similar variation, increasing with increasing BT concentration up to a maximum at a composition near the MPB and then decreasing. The piezoelectric constant attains a maximum value of 176 pC/N at $x = 0.07$ and the electromechanical coupling factor reaches a maximum value of 25.5% at $x = 0.06$. With respect to both the piezoelectric constant and electromechanical coupling factor, the composition of $x = 0.07$ shows preferred piezoelectric properties, with a piezoelectric constant

Table 1
Phase compositions of NBT–(*x*)BT ceramics

Sample	Peak	Peak area (S)	Peak area of rhombohedral phase $S_{(202)}$	Peak area of tetragonal phase $S_{(200)} + S_{(002)}$	M_R(%)
$x = 0.06$	(200)	1089.32	950.13	1089.32	46.6
	(202)	950.13			
	(002)	0.00			
$x = 0.07$	(200)	585.63	588.79	1040.19	36.2
	(202)	588.79			
	(002)	454.55			
$x = 0.08$	(200)	360.91	464.25	1010.71	31.5
	(202)	464.25			
	(002)	649.79			
$x = 0.10$	(200)	216.71	93.41	1609.51	5.5
	(202)	93.41			
	(002)	1392.78			

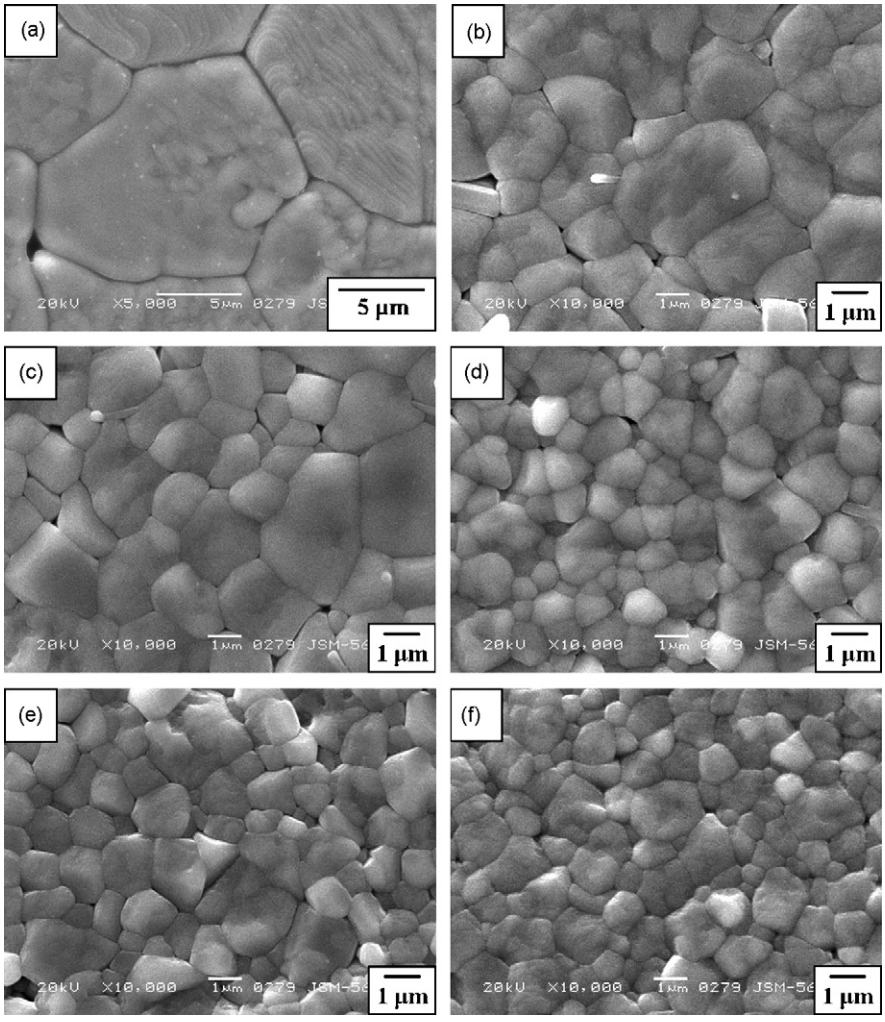

Fig. 3. SEM micrographs of NBT–(*x*)BT ceramics with (a) $x = 0$, (b) $x = 0.02$, (c) $x = 0.04$, (d) $x = 0.07$, (e) $x = 0.08$ and (f) $x = 0.12$.

of 176 pC/N and a relatively high electromechanical coupling factor of 21.2% simultaneously, where the relative content of the tetragonal phase is substantially higher than that of the rhombohedral phases according to the Table 1.

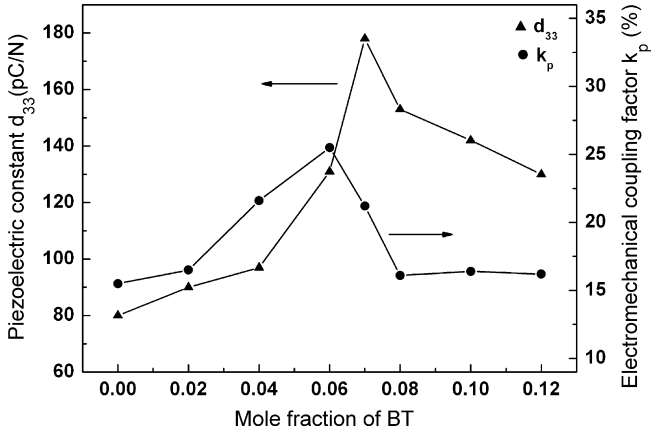

Fig. 4. Piezoelectric properties of NBT–(*x*)BT ceramics as a function of BT concentration.

It was reported that the piezoelectric constant and electromechanical coupling factor of NBT–(*x*)BT ceramics made by the conventional solid-state method reach maximum values of $d_{33} = 122$ pC/N and $k_p = 29.0\%$ at $x = 0.06$.[6] In our study, the piezoelectric properties for the specimens of $x = 0.06$ are roughly compatible with the previously reported values. However, there is a discrepancy between the result of the present work and the previous research in the composition where the piezoelectric constant attains its maximum value. This can be ascribed to the effect of fabrication process on the piezoelectric properties.[17] Besides, the piezoelectric constant of the specimen with $x = 0.07$ is also apparently larger than the maximum values (149 and 152 pC/N) of NBT–(*x*)BT ceramics made by the conventional solid-state method with oxide additives introduced as modifier, which were regarded as the largest piezoelectric constant values obtained so far in NBT–(*x*)BT ceramics.[6,18] Therefore, we can infer that compared with conventional preparation method, the citrate method is an viable and advantageous route to the production of NBT–(*x*)BT piezoelectric ceramics. This can probably be attributed to two main factors: the fineness of the powders synthesized by the citrate method and their chemical stoichiometry. On the one hand, uniform morphology and high purity of

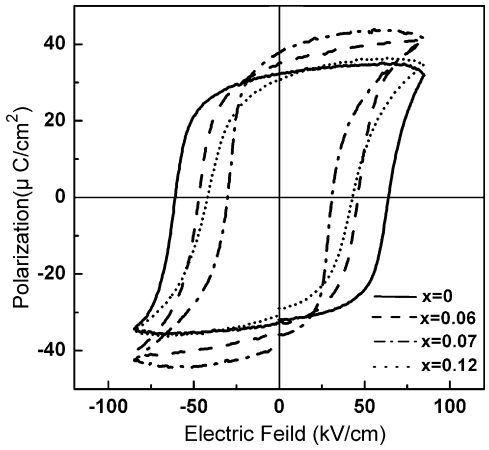

Fig. 5. P–E hysteresis loops of NBT–(*x*)BT ceramics at room temperature.

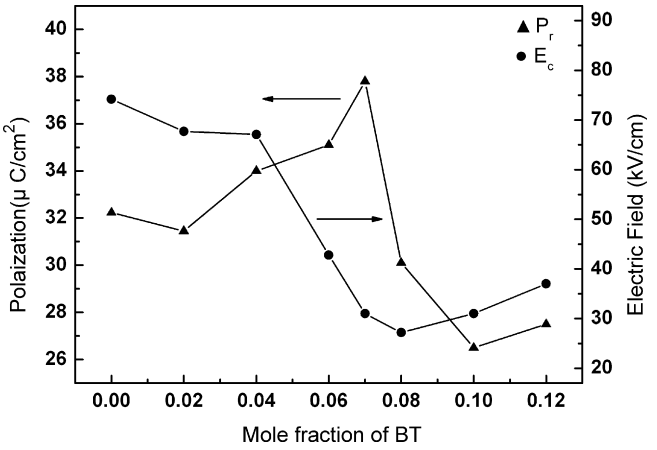

Fig. 6. Remanent polarization and coercive field of NBT–(*x*)BT ceramics as a function of BT concentration.

the powders synthesized by the citrate method is advantageous for the enhancement of the piezoelectric properties of the resulting ceramic specimens. On the other hand, Fig. 6 shows that the piezoelectric properties of NBT–(*x*)BT compositions near the MPB are rather sensitive to the phase composition. Given that it allows the chemical stoichiometry to be controlled in a more accurately way, the citrate method is more superior to the conventional solid-state method.

Saturated P–E hysteresis loops were observed over the whole investigated compositional range. Fig. 5 shows the typical P–E hysteresis loops of NBT–(*x*)BT ceramics at room temperature, from which the remanent polarization (P_r) and the coercive field (E_c) values were derived. Fig. 6 shows the remanent polarization (P_r) and coercive field (E_c) values of NBT–(*x*)BT ceramics as a function of the BT concentration. The remanent polarization

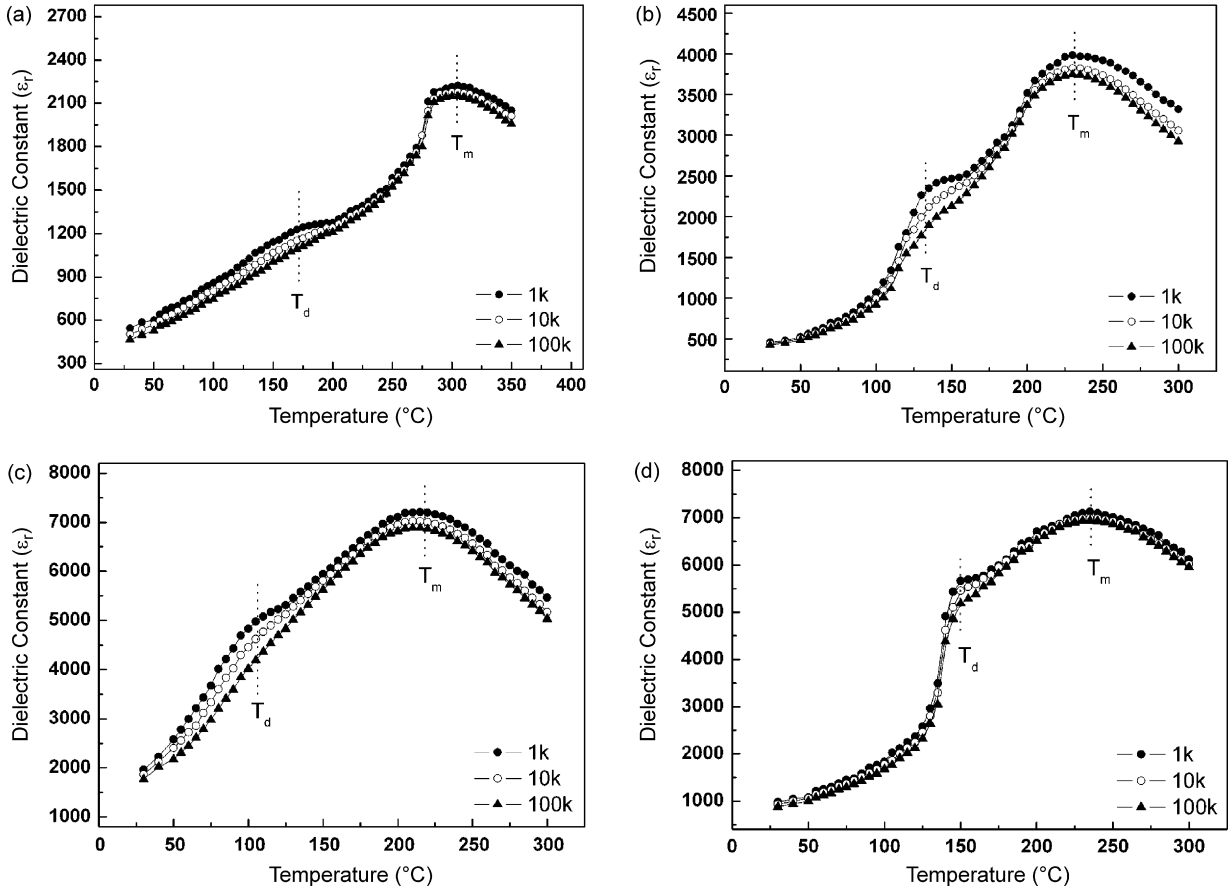

Fig. 7. Temperature dependence of dielectric constant for NBT–(*x*)BT ceramics at frequencies ranging from 1 to 100 kHz with (a) $x = 0$, (b) $x = 0.02$, (c) $x = 0.07$ and (d) $x = 0.12$.

of the specimens increases with increasing BT concentration up to a maximum of $P_r = 37.8\,\mu C/cm^2$ at $x = 0.07$ and then decreases, while the coercive field decreases with increasing BT concentration to a minimum of $E_c = 27.2\,kV/cm$ at $x = 0.08$ and then increases slightly. This is generally consistent with the variation of the piezoelectric properties with BT concentration and indicates an essential relation between the ferroelectric and piezoelectric properties of NBT–(x)BT ceramics. The specimen with $x = 0.07$ exhibits the maximum remanent polarization and a relatively low coercive field, which are presumably responsible for its superior piezoelectric properties.

Fig. 7 shows the temperature dependence of the dielectric constant (ε_r) for NBT–(x)BT ceramics at frequencies ranging from 1 to 100 kHz. For each specimen, two abnormal dielectric peaks are observed during the heating process. The temperature corresponding to the peak in the low temperature range is denoted as depolarization temperature (T_d), which has been suggested to be an indication of the stability of the ferroelectric domains.[6] The temperature corresponding to the maximum value of dielectric constant is referred to as the maximum temperature (T_m) or Curie point (T_c).[6] Fig. 8 shows the piezoelectric constants and depolarization temperatures of NBT–(x)BT ceramics as a function of BT concentration. The MPB compositions exhibit a lower depolarization temperature, which implies a reduction of the stability of ferroelectric domains. Compared with the compositions consisting of one single phase, the coexistence of a mixed rhombohedral–tetragonal phase could lead to more powerful stress in the MPB compositions, due to the incompatibility of their crystal lattices, resulting in a decrease of the thermal stability in the long-range ferroelectric domains.[19,20] This can be regarded as the origin of the lower depolarization temperature at the MPB compositions.

It is well-known that pure NBT has relaxor characteristics and shows peculiar behavior of the diffuse phase transition from ferroelectric rhombohedral to nonpolar tetragonal transition.[21] In this study, the typical relaxor behavior of NBT–(x)BT ceramics is characterized by a diffuse ferroelectric phase transition, with two broad peaks and a strong frequency dependence of the dielectric constant. A modified Curie–Weiss

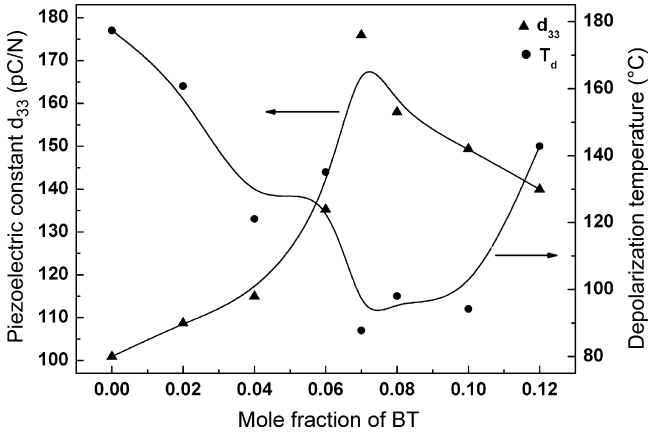

Fig. 8. Piezoelectric constants and depolarization temperatures of NBT–(x)BT ceramics as a function of the BT concentration.

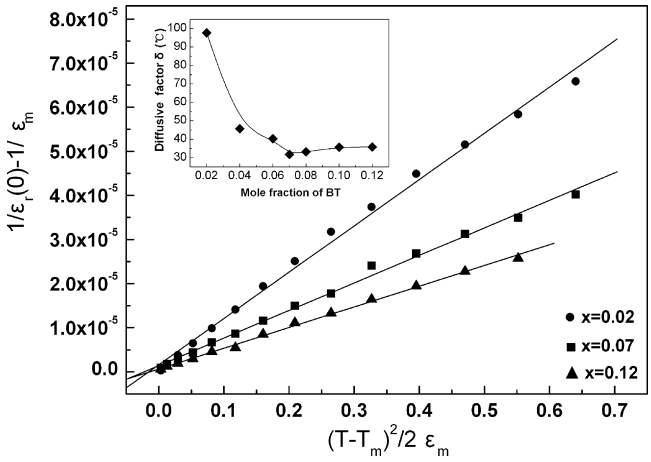

Fig. 9. The plots of $(1/\varepsilon_r - 1/\varepsilon_{r\,max})$ as function of $(T - T_m)^2/2\varepsilon_{r\,max}$ for the three selected samples ($x = 0.02$, 0.07 and 0.12). The inset shows the composition dependence of diffusive factor.

law has been proposed to quantify the diffuseness of a phase transition[22]:

$$\frac{1}{\varepsilon_r} = \frac{1}{\varepsilon_{r\,max}} + \frac{(T - T_m)^2}{2\varepsilon_{r\,max}\delta^2}$$

where $\varepsilon_{r\,max}$ is the maximum permittivity and T_m is the Curie point.[22] The values of the diffusive factor (δ) can be obtained from the slope of the plots of $1/\varepsilon_r$ versus $(T - T_m)^2$. Fig. 9 shows the plots of $(1/\varepsilon_r - 1/\varepsilon_{r\,max})$ as function of $(T - T_m)^2/2\varepsilon_{r\,max}$ for the three selected samples ($x = 0.02$, 0.07 and 0.12). The substitution of Ba^{2+} for $(Na_{0.5}Bi_{0.5})^{2+}$ in the A-site of the perovskite structure is the main factor that induces some order in the cationic octahedral sublattice due to the large difference in the shannon radii between Ba^{2+}(1.35 Å) and $(Na_{0.5}Bi_{0.5})^{2+}$(0.97 Å),[23,24] and then produces a decease of the diffusive factor as increasing BT concentration. These result imply a degradation of the relaxor feature and a transition from relaxor ferroelectrics to normal ferroelectrics.

4. Conclusions

The citrate method was found to be an advantageous alternative to the conventional method to produce $(Na_{0.5}Bi_{0.5})_{1-x}Ba_xTiO_3$ piezoelectric ceramics. The powders synthesized by the citrate method consist of homogeneous and fine particles. The resulting $(Na_{0.5}Bi_{0.5})_{1-x}Ba_xTiO_3$ ceramics exhibit superior piezoelectric properties near the rhombohedral–tetragonal morphotropic phase boundary. The piezoelectric constant attains a maximum values of $d_{33} = 176\,pC/N$ at $x = 0.07$, corresponding to a relatively large remanent polarization of $P_r = 37.8\,\mu C/cm^2$ and a relatively low coercive field of $E_c = 27.2\,kV/cm$. $(Na_{0.5}Bi_{0.5})_{1-x}Ba_xTiO_3$ ceramics present a decrease of phase diffuse factor (δ) with increasing $BaTiO_3$ content, implying a degradation of the relaxor feature and a transition from relaxor ferroelectrics to normal ferroelectrics.

Acknowledgements

This work was financially supported by the Program for New Century Excellent Talents in University of China (Grant No. NCET-04-0724) and the Program for the Training of Graduate Students in Regional Innovation which was conducted by the Ministry of Commerce Industry and Energy of the Korean Government. We are grateful to the NSFC (50272044 and 50410529) and the KOSEF (F01-2004-000-10084-0) for jointly supporting this research.

References

1. Smolenskii, G. A., Isupov, V. A., Agranovskaya, A. I. and Krainik, N. N., New ferroelectrics of complex composition. *Sov. Phys. Solid State (Engl. Transl.)*, 1961, **2**, 2651–2654.
2. Takenaka, T., Maruyama, K. and Sakata, K., $(Bi_{1/2}Na_{1/2})TiO_3$–$BaTiO_3$ system for lead-free piezoelectric ceramics. *Jpn. J. Appl. Phys.*, 1991, **30**(9B), 2236–2239.
3. Ichinose, N. and Udagawa, K., Piezoelectric properties of $(Bi_{1/2}Na_{1/2})TiO_3$-based ceramics. *Ferroelectrics*, 1995, **169**, 317–325.
4. Takenaka, T., Okuda, T. and Takegahara, K., Lead-free piezoelectric ceramics based on $(Bi_{1/2}Na_{1/2})TiO_3$–$NaNbO_3$. *Ferroelectrics*, 1997, **196**, 175–178.
5. Takenaka, T., Piezoelectric properties of some lead-free ferroelectric ceramics. *Ferroelectrics*, 1999, **230**, 87–98.
6. Chu, B. J., Chen, D. R., Li, G. R. and Yin, Q. R., Electrical properties of $(Na_{1/2}Bi_{1/2})TiO_3$–$BaTiO_3$ ceramics. *J. Eur. Ceram. Soc.*, 2002, **22**, 2115–2121.
7. Elkechai, O., Manier, M. and Mercurio, J. P., $Bi_{0.5}Na_{0.5}TiO_3$–$Bi_{0.5}K_{0.5}TiO_3$ system: a structure and electrical study. *Phys. Status Solid (a)*, 1996, **157**, 499–506.
8. Ramana, E. V., Saradhi, B. V., Suryanarayana, S. V. and Bhimasankaram, T., Synthesis and characterisation of $(1-x)Na_{1/2}Bi_{1/2}TiO_3$–$x$$BiFeO_3$ ceramics. *Ferroelectrics*, 2005, **324**, 55–61.
9. Lin, D. M., Xiao, D. Q., Zhu, J. G. and Yu, P., Piezoelectric and ferroelectric properties of $[Bi_{0.5}(Na_{1-x-y}K_xLi_y)_{0.5}]TiO_3$ lead-free piezoelectric ceramics. *Appl. Phys. Lett.*, 2006, **88**, 062901-1-062901-3.
10. West, D. L. and Payne, D. A., Preparation of $0.95Bi_{1/2}Na_{1/2}TiO_3$–$0.05BaTiO_3$ ceramics by an aqueous citrate–gel route. *J. Am. Ceram. Soc.*, 2003, **86**, 192–194.
11. Kim, B. H., Han, S. J., Kim, J. H., Lee, J. H., Ahn, B. K. and Xu, Q., Electrical properties of $(1-x)$ (Bi0.5Na0.5)TiO3–xBaTiO3 synthesized by emulsion method. *Ceram. Int.*, 2007, **33**, 447–452.
12. Pookmanee, P., Rujijanagul, G., Ananta, S., Heimann, R. B. and Phanichphant, S., Effect of sintering temperature on microstructure of hydrothermally prepared bismuth sodium titanate ceramics. *J. Eur. Ceram. Soc.*, 2004, **24**, 517–520.
13. Hao, J. J., Wang, X. H., Chen, R. Z. and Li, L. T., Synthesis of (Bi0.5Na0.5)TiO3 nanocrystalline powders by stearic acid gel method. *Mater. Chem. Phys.*, 2005, **90**, 282–285.
14. Zhao, M. L., Wang, C. L., Zhong, W. L., Wang, J. F. and Chen, H. C., Electrical properties of $(Bi_{0.5}Na_{0.5})TiO_3$ ceramic prepared by sol–gel method. *Acta. Phys. Sin. -Chin. Ed.*, 2003, **52**, 229–233.
15. Xu, Q., Chen, X. L., Chen, W., Chen, M., Xu, S. L., Kim, B. H. *et al.*, Effect of MnO addition on structure and electrical properties of $(Na_{0.5}Bi_{0.5})_{0.94}Ba_{0.06}TiO_3$ ceramics prepared by citrate method. *Mater. Sci. Eng. B*, 2006, **130**, 94–100.
16. Cao, W. W. and Cross, L. E., Theoretical model for the morphotropic phase boundary in lead zirconate-lead titanate solid solution. *Phys. Rev. B*, 1993, **47**, 4825–4830.
17. Park, S. E. and Hong, K. S., Phase relations in the system of $(Na_{0.5}Bi_{0.5})TiO_3$–$PbTiO_3$ I. *Structure*, 1996, **79**, 383–387.
18. Wang, X. X., Chan, H. L. W. and Choy, C. L., Piezoelectric and dielectric properties of CeO-added $(Na_{0.5}Bi_{0.5})_{0.94}Ba_{0.06}TiO_3$ lead-free ceramics. *Solid State Commun.*, 2003, **125**, 395–399.
19. Dai, X. H., Digiovanni, A. and Viehland, D., Dielectric properties of tetragonal lanthanum modified lead zirconate titanate ceramics. *J. Appl. Phys.*, 1993, **74**, 3399–3405.
20. Yoon, M. S., Jang, H. M. and Kim, S., Spontaneous micro–macro ferroelectric domain switching in $PbZrO_3$-doped $Pb(Ni_{1/3}Nb_{2/3})O_3$–$PbTiO_3$ system. *Jpn. J. Appl. Phys.*, 1995, **4**, 1916–1921.
21. Tu, C. S., Siny, I. G. and Schmidt, V. H., Sequence of dielectric anomalies and high-temperature relaxation behavior in $Na_{1/2}Bi_{1/2}TiO_3$. *Phys. Rev. B.*, 1994, **49**, 550–559.
22. Xia, F. and Yao, X., Piezoelectric and dielectric properties of PZN-BT-PZT solid solutions. *J. Mater. Sci.*, 1999, **34**, 3341–3343.
23. Chu, B. J., Li, G. R., Jiang, X. P. and Chen, D. R., Piezoelectric property and relaxation phase transition of $Na_{1/2}Bi_{1/2}TiO_3$–$BaTiO_3$ system. *J. Inorg. Mater.*, 2000, **15**, 815–821.
24. Setter, N. and Cross, L.E., The role of B-site cation disorder in diffuse phase transition behavior of perovskite ferroelectrics, J. Appl. Phys., 1980, **51**, 4356–4360.